Nonooperative Containment Control for Multiple Unmanned Surface Vehicles With Improved Extended State Observer

Wentao Wu [1,2], Zhenhua Li [1,2], Yibo Zhang [2], and Weidong Zhang [2,3]

1. SJTU Sanya Yazhou Bay Institute of Deepsea Science and Technology, Hainan, 5720hai 200240, China

2. Department of Automation, Shanghai Jiao Tong University, Shanghai 200240, China

3. School of Information and Communication Engineering, Hainan University, Haikou 570228, Hainan, China
E-mail: {wentao-wu, lizhenhuagd, zhang297, wdzhang}@sjtu.edu.cn

Abstract: This paper investigates a distributed containment control problem of multiple autonomous surface vehicles (ASVs) in the presence of internal and external disturbances. Considering some ASVs with individual tasks, a noncooperative game-based control scheme is developed to achieve the containment behavior of multiple ASVs. To deal with the internal and external disturbances, we design an improved extended state observer (IESO). Using the Nash equilibrium seeking strategy, an IESO-based noncooperative containment controller is presented. It is proved that the closed-loop system is input-to-state stable, and position and heading of all ASVs converge to the Nash equilibrium as far as possible. Finally, simulation results are given to demonstrate the effectiveness of proposed scheme.

Key Words: Multiple unmanned surface vehicles, containment control, noncooperative game, and improved extended state observer

1 Introduction

Inspired by the natural biological swarm, the cooperative behavior of autonomous surface vehicles (ASVs) has attracted increasing attention and interest from research institutes and communities [1–6]. The cooperative control architecture of ASVs is divided into the centralized control, decentralized control, and distributed control [7]. In the distributed architecture, the local control law is used for each subsystem without relying on global information [8–10]. A typical distributed architecture is the containment control separated into containment tracking [11–13] and containment maneuvering [14–16]. In particular, containment tracking control aims to form a convex shape of multiple ASVs guided by multiple virtual leaders.

On the one hand, these containment control methods in [11–14, 16, 17] mainly concern how to establish the desired collaborative behavior via the local cooperation among ASVs. It is noted that there may exist a competition relationship among ASVs besides cooperation in practice. The competition means that some ASVs have individual tasks, which will result in challenges for the implementation of group tasks. Noncooperative game theory is an effective tool to handle the conflict of multiple ASVs in competition and cooperation. Based on the noncooperative game, an appreciative decision can be made for every ASV with the Nash equilibrium (NE) seeking strategy [18]. Up to now, there are some NE seeking results for consensus control of multiple ASVs (see [19–22]). It is found that [19–22] consider the NE seeking for a group of ASVs guided by one leader. There is seldom the NE seeking result of ASVs guided by multiple leaders.

On the other hand, the dynamics of ASVs are subject to modeling errors, unmodeled terms, and environmental disturbances in practice. References [19, 20] designed the static formation controller with known ASV's kinetics. In [21, 22], environmental disturbances are considered and recovered by constructing the neural predictors or data-driven observers. Motivated by the above discussion, the main highlights of this paper are given as follows: 1) To deal with unknown disturbances for ASVs, an improved extended state observer (IESO) is presented to overcome the chattering of compensated controller; 2) An IESO-based noncooperative containment control scheme is developed for multiple ASVs by using the NE seeking strategy, which can achieve the balance between the individual and group objectives.

2 Preliminaries and Problem Formulation

2.1 Notation

The Euclidean norm is denoted by $\|\cdot\|$. $\lambda_{\min}(\cdot)$ and $\lambda_{\max}(\cdot)$ are minimum and maximum eigenvalues of a matrix. An m-dimensional zero vector and an $m \times n$ dimensional zero matrix are represented by $\mathbf{0}_m$ and $\mathbf{0}_{m\times n}$. $\mathrm{col}(\cdot)$ and $\mathrm{diag}(\cdot)$ represent a column vector and a diagonal matrix, respectively. $\otimes$ is the Kronecker Product.

2.2 Graph theory

A graph $\mathcal{G} = \{\mathcal{V}, \mathcal{E}\}$ is used to describe the communication topology. $\mathcal{V} = \{\mathcal{V}_F, \mathcal{V}_L\}$ is a node set of M follower nodes and $N - M$ leader nodes. $\mathcal{E}$ denotes an edge set $\mathcal{E} = \{(i, j) \in \mathcal{V} \times \mathcal{V}\}$, where the node pairs (i, j) stands for a transformation path from node i to node j with a weight $a_{ij} = 1$ or $a_{ij} = 0$. If $a_{ij} = a_{ji}$, the graph is called an undirected graph. A square matrix $\boldsymbol{\mathcal{A}} = [a_{ij}] \in \Re^{N\times N}$ is an adjacency matrix of graph $\mathcal{G}$. An in-degree matrix $\boldsymbol{\mathcal{D}} \in \Re^{N\times N}$ is given with diagonal element $\sum_{j\in\mathcal{V}} a_{ij}$. Then, a Laplacian matrix $\boldsymbol{\mathcal{L}} \in \Re^{N\times N}$ is presented by $\boldsymbol{\mathcal{L}} = \boldsymbol{\mathcal{D}} - \boldsymbol{\mathcal{A}}$.

This work was supported in part by the Hainan Special Ph.D. Scientific Research Foundation of Sanya Yazhou Bay Science and Technology City under Grant HSPHDSRF-2022-01-007 and Grant HSPHDSRF-2022-01-005; in part by the National Key R&D Program of China under Grant 2022ZD0119900; in part by the Shanghai Science and Technology Program under Grant 22015810300; in part by the Hainan Province Science and Technology Special Fund under Grant ZDYF2021GXJS041; in part by the National Natural Science Foundation of China under Grant U2141234 and Grant 52201369. (Corresponding author: Weidong Zhang.)

2023 China Automation Congress (CAC) | 979-8-3503-0375-9/23/$31.00 ©2023 IEEE | DOI: 10.1109/CAC59555.2023.10451380

979-8-3503-0375-9/23/$31.00 ©2023 IEEE Authorized licensed use limited to: Shanghai Jiaotong University. Downloaded on December 22,2024 at 11:13:09 UTC from IEEE Xplore. Restrictions apply.

2.3 Problem Formulation

In this paper, we consider the noncooperative game-based containment control of M ASVs and $N-M$ virtual leaders. In the containment, virtual leaders span a hull to coordinate the motions of multiple ASVs. The action of each ASV is given by

$$\begin{aligned} \dot{\boldsymbol{\eta}}_i &= \boldsymbol{R}_i(\psi_i)\boldsymbol{\nu}_i, \\ \boldsymbol{M}_i\dot{\boldsymbol{\nu}}_i + \boldsymbol{C}_i(\boldsymbol{\nu}_i)\boldsymbol{\nu}_i + \boldsymbol{D}_i(\boldsymbol{\nu}_i)\boldsymbol{\nu}_i &= \boldsymbol{\tau}_i + \boldsymbol{\tau}_{i\omega}, \end{aligned} \tag{1}$$

where $i = 1, \ldots, M$. $\boldsymbol{\eta}_i = [x_i, y_i, \psi_i]^T \in \Re^3$ denotes a position and yaw angle in the earth-fixed reference frame. $\boldsymbol{\nu}_i = [u_i, v_i, r_i]^T \in \Re^3$ is a velocity vector in the body-fixed reference frame. $\boldsymbol{M}_i = \boldsymbol{M}_i^T \in \Re^{3\times 3}$, $\boldsymbol{C}_i(\boldsymbol{\nu}_i) = -\boldsymbol{C}_i^T(\boldsymbol{\nu}_i) \in \Re^{3\times 3}$, and $\boldsymbol{D}_i(\boldsymbol{\nu}_i) \in \Re^{3\times 3}$ represent an inertial mass matrix, a Coriolis/centripetal matrix, and a damping matrix, respectively. $\boldsymbol{\tau}_i \in \Re^3$ is the actual control input. $\boldsymbol{\tau}_{i\omega} \in \Re^3$ denotes the disturbance vector. $\boldsymbol{R}_i(\psi_i)$ is a rotation matrix described by

$$\boldsymbol{R}_i(\psi_i) = \boldsymbol{R}_i = \begin{bmatrix} \cos\psi_i & -\sin\psi_i & 0 \\ \sin\psi_i & \cos\psi_i & 0 \\ 0 & 0 & 1 \end{bmatrix}.$$

In this paper, ASVs are viewed as a group of players that built a set defined as $\mathcal{V}_F = \{1, 2, ..., M\}$. For a noncooperative game, each player intends to minimize its objective function $f_i(\boldsymbol{\eta}_F) : \Re^{3M} \to \Re$, i.e.

$$\begin{aligned} \min_{\boldsymbol{\eta}_i \in \Re^3} \quad & f_i(\boldsymbol{\eta}_F) \\ \text{subject to} \quad & (1) \end{aligned} \tag{2}$$

where $\boldsymbol{\eta}_F = \mathrm{col}(\boldsymbol{\eta}_i)$, $i \in \mathcal{V}_F$. It is seen that $f_i(\boldsymbol{\eta}_F)$ is depended on the actions of the ith player and its neighbors in the considered game. Then, the ith player can adjust its action $\boldsymbol{\eta}_i$ to minimize the function $f_i(\boldsymbol{\eta}_F)$. Thus, an action profile $\boldsymbol{\eta}_F^* = (\boldsymbol{\eta}_i^*, \boldsymbol{\eta}_{-i}^*)$ is given and called as a Nash equilibrium if for $\boldsymbol{\eta}_i \in \Re^3$,

$$f_i(\boldsymbol{\eta}_i, \boldsymbol{\eta}_{-i}^*) \geq f_i(\boldsymbol{\eta}_i^*, \boldsymbol{\eta}_{-i}^*),\ i \in \mathcal{V}_F \tag{3}$$

with $\boldsymbol{\eta}_{-1}^* = [\boldsymbol{\eta}_1^{*T}, ..., \boldsymbol{\eta}_{i-1}^{*T}, \boldsymbol{\eta}_{i+1}^{*T}, \boldsymbol{\eta}_M^{*T}]^T$. In addition, if $f_i(\boldsymbol{\eta}_F)$ is convex and continuous, there is a Nash equilibrium of noncooperative game such that $\partial J_i(\boldsymbol{\eta}_F^*)/\partial \boldsymbol{\eta}_i = \boldsymbol{0}_3$.

This paper aims to develop the controller to achieve a containment behavior of multiple ASVs guided by virtual leaders. In the noncooperative game, each ASV intends to complete the following objectives:

$$\text{Objective1: } \min \Sigma_{j\in\mathcal{N}_{iF}} a_{ij}\|\boldsymbol{\eta}_i - \boldsymbol{\eta}_j\|^2, \tag{4}$$

$$\text{Objective2: } \min \Sigma_{k\in\mathcal{N}_{iL}} a_{ik}\|\boldsymbol{\eta}_i - \boldsymbol{\eta}_{kd}\|^2, \tag{5}$$

where $\boldsymbol{\eta}_{kd} = [x_{kd}, y_{kd}, \psi_{kd}] \in \Re^3$, $k \in \mathcal{V}_L$ with $\psi_{kd} = \mathrm{atan2}(\dot{y}_{kd}, \dot{x}_{kd})$ denotes the desired reference trajectory. Note that some ASVs intend to minimize the containment errors with their neighboring ASVs and virtual leaders. In the upcoming section, the following assumptions will be needed.

Assumption 1: The graph for ASVs and virtual leaders is undirected and connected. There exists at least one ASV accessing the information of virtual leaders.

Assumption 2: The given trajectory $\boldsymbol{\eta}_{kd}$ and its derivatives $\dot{\boldsymbol{\eta}}_{kd}$ and $\ddot{\boldsymbol{\eta}}_{kd}$ are bounded and satisfied with $\|\boldsymbol{\eta}_{kd}\| \leq \epsilon_1 \in \Re^+$, $\|\dot{\boldsymbol{\eta}}_{kd}\| \leq \epsilon_2 \in \Re^+$, and $\|\ddot{\boldsymbol{\eta}}_{kd}\| \leq \epsilon_3 \in \Re^+$.

3 Main Results

In this section, we consider a noncooperative game-based containment control of multiple ASVs subject to unknown internal uncertainties and external disturbances.

3.1 Improved Extended State Observer Design

To facilitate to the subsequent strategy design, define $\boldsymbol{\sigma}_i(\boldsymbol{\nu}_i) = \boldsymbol{M}_i^{-1}(-\boldsymbol{C}_i(\boldsymbol{\nu}_i)\boldsymbol{\nu}_i - \boldsymbol{D}_i(\boldsymbol{\nu}_i)\boldsymbol{\nu}_i + \boldsymbol{\tau}_{i\omega})$. Then, it yields the dynamics of the ith ASV's action as follows:

$$\begin{cases} \dot{\boldsymbol{\eta}}_i = \boldsymbol{R}(\psi_i)\boldsymbol{\nu}_i, \\ \dot{\boldsymbol{\nu}}_i = \boldsymbol{z}_i + \boldsymbol{M}_i^{-1}\boldsymbol{\tau}_i, \\ \dot{\boldsymbol{z}}_i = \dot{\boldsymbol{\sigma}}_i \end{cases} \tag{6}$$

with $\boldsymbol{z}_i = \boldsymbol{\sigma}_i(\boldsymbol{\nu}_i)$ being regarded as an extended state.

For ASVs with the measurable velocity $\boldsymbol{\nu}_i$, a second-order IESO is derived to estimate the unavailable $\boldsymbol{z}_i$

$$\begin{cases} \tilde{\boldsymbol{\nu}}_i = \hat{\boldsymbol{\nu}}_i - \boldsymbol{\nu}_i, \\ \dot{\tilde{\boldsymbol{\nu}}}_i = -l_{i1}\mathbf{tanh}(\tilde{\boldsymbol{\nu}}_i) + \hat{\boldsymbol{z}}_i(\boldsymbol{\nu}_i) + \boldsymbol{M}_i^{-1}\boldsymbol{\tau}_i, \\ \dot{\hat{\boldsymbol{z}}}_i = -l_{i2}\mathbf{tanh}(\tilde{\boldsymbol{\nu}}_i), \end{cases} \tag{7}$$

where $\hat{\boldsymbol{\nu}}_i$ and $\hat{\boldsymbol{z}}_i$ represent the estimations of $\boldsymbol{\nu}_i$ and $\boldsymbol{z}_i$, respectively. $\tilde{\boldsymbol{\nu}}_i$ represents the velocity estimation error. $l_{i1} \in \Re^+$ and $l_{i2} \in \Re^+$ are observer coefficients. $\mathbf{tanh}(\tilde{\boldsymbol{\nu}}_i) = \mathrm{col}(\tanh(\tilde{\nu}_{ij}))_{,j=u,v,r}$ is a smooth function vector with

$$\tanh(\tilde{\nu}_{ij}) = \begin{cases} b_0 \dfrac{e^{c_0|\tilde{\nu}_{ij}|} - \mathrm{e}^{-c_0|\tilde{\nu}_{ij}|}}{e^{c_0|\tilde{\nu}_{ij}|} + e^{-c_0|\tilde{\nu}_{ij}|}} \dfrac{\tilde{\nu}_{ij}}{|\tilde{\nu}_{ij}|}, & \tilde{\nu}_{ij} \neq 0, \\ \tilde{\nu}_{ij}, & \tilde{\nu}_{ij} = 0, \end{cases}$$

where b_0 and c_0 are positive constants.

Define a positive vector $\boldsymbol{\zeta}_i = \mathrm{diag}\{\zeta_{ij}\}_{,j=u,v,r}$ with

$$\zeta_{ij} = \begin{cases} b_0 \dfrac{e^{c_0|\tilde{\nu}_{ij}|} - \mathrm{e}^{-c_0|\tilde{\nu}_{ij}|}}{e^{c_0|\tilde{\nu}_{ij}|} + e^{-c_0|\tilde{\nu}_{ij}|}} |\tilde{\nu}_{ij}^{-1}|, & \tilde{\nu}_{ij} \neq 0, \\ 1, & \tilde{\nu}_{ij} = 0. \end{cases} \tag{8}$$

Then, IESO (7) using (8) can be rewritten as follows

$$\begin{cases} \dot{\tilde{\boldsymbol{\nu}}}_i = -l_{i1}\boldsymbol{\zeta}_i\tilde{\boldsymbol{\nu}}_i + \hat{\boldsymbol{z}}_i + \boldsymbol{M}_i^{-1}\boldsymbol{\tau}_i, \\ \dot{\tilde{\boldsymbol{z}}}_i = -l_{i2}\boldsymbol{\zeta}_i\tilde{\boldsymbol{\nu}}_i. \end{cases} \tag{9}$$

Integrating (6) and (9), it obtains the dynamics of estimated errors as follows

$$\begin{cases} \dot{\tilde{\boldsymbol{\nu}}}_i = -l_{i1}\boldsymbol{\zeta}_i\tilde{\boldsymbol{\nu}}_i + \tilde{\boldsymbol{z}}_i, \\ \dot{\tilde{\boldsymbol{z}}}_i = -l_{i2}\boldsymbol{\zeta}_i\tilde{\boldsymbol{\nu}}_i - \dot{\boldsymbol{z}}_i \end{cases} \tag{10}$$

with $\tilde{\boldsymbol{z}}_i = \hat{\boldsymbol{z}}_i - \boldsymbol{z}_i$.

Letting $\boldsymbol{E}_{i1} = [\tilde{\boldsymbol{\nu}}_i^T, \tilde{\boldsymbol{z}}_i^T]^T$, it follows from (10)

$$\dot{\boldsymbol{E}}_{i1} = \boldsymbol{A}_{i1}\boldsymbol{E}_{i1} - \boldsymbol{B}_{i1}\dot{\boldsymbol{z}}_i, \tag{11}$$

where $\boldsymbol{A}_{i1} = \begin{bmatrix} -l_{i1}\boldsymbol{\zeta}_i & \boldsymbol{I}_3 \\ -l_{i2}\boldsymbol{\zeta}_i & \boldsymbol{0}_{3\times 3} \end{bmatrix}$, $\boldsymbol{B}_{i1} = \begin{bmatrix} \boldsymbol{0}_{3\times 3} \\ \boldsymbol{I}_3 \end{bmatrix}$.

Since $\zeta_{ij} > 0$ from definition in (8), it gets that $\boldsymbol{A}_{i1}$ is a Hurwitz matrix. Then, there exists a matrix $\boldsymbol{P}_{i1} = \boldsymbol{P}_{i1}^T > 0$ such that

$$\boldsymbol{A}_{i1}^T\boldsymbol{P}_{i1} + \boldsymbol{P}_{i1}\boldsymbol{A}_{i1} = -\boldsymbol{I}_6. \tag{12}$$

Assumption 3: The derivative of $\boldsymbol{\sigma}_i$ is bounded and satisfied with $\|\dot{\boldsymbol{\sigma}}_i\| \leq \sigma^* \in \Re^+$.

Lemma 1 ([23]): Under Assumption 3, the subsystem (11) is stable and estimated errors are bounded.

Authorized licensed use limited to: Shanghai Jiaotong University. Downloaded on December 22,2024 at 11:13:09 UTC from IEEE Xplore. Restrictions apply.

3.2 Noncooperative Containment Controller Design

In the previous section, the unknown disturbance of ASVs can be recovered using designed IESO. This will develop an IESO-based noncooperative containment controller for ASVs in the presence of internal and external disturbances.

This paper considers a noncooperative game for containment tracking of M ASVs guided by $N-M$ virtual leaders. First, an objective function f_i including the individual task and swarm task is defined as

$$f_i(\boldsymbol{\eta}_F) = \frac{1}{2}\sum_{j\in\mathcal{N}_{iF}} a_{ij}\|\boldsymbol{\eta}_i-\boldsymbol{\eta}_j\|^2+\frac{1}{2}\sum_{k\in\mathcal{N}_{iL}} a_{ik}\|\boldsymbol{\eta}_i-\boldsymbol{\eta}_{kd}\|^2. \quad (13)$$

According to (13), it takes the partial derivative of $f_i(\boldsymbol{\eta}_F)$ with respect to $\boldsymbol{\eta}_i$ as

$$\begin{aligned}\boldsymbol{\nabla}_i(\boldsymbol{\eta}_F) &= \frac{\partial f_i(\boldsymbol{\eta}_F)}{\partial \boldsymbol{\eta}_i}\\ &= \sum_{j\in\mathcal{N}_{iF}} a_{ij}(\boldsymbol{\eta}_i-\boldsymbol{\eta}_j)+\sum_{k\in\mathcal{N}_{iL}} a_{ik}(\boldsymbol{\eta}_i-\boldsymbol{\eta}_{kd}).\end{aligned} \quad (14)$$

Denoting $\boldsymbol{\nabla}(\boldsymbol{\eta}_F) = \mathrm{col}(\boldsymbol{\nabla}_i(\boldsymbol{\eta}_F))$, $i\in\mathcal{V}_F$, it follows from (14)

$$\boldsymbol{\nabla}(\boldsymbol{\eta}_F) = (\boldsymbol{\mathcal{L}}_1\otimes\boldsymbol{I}_3)\boldsymbol{\eta}_F+(\boldsymbol{\mathcal{L}}_2\otimes\boldsymbol{I}_3)\boldsymbol{\eta}_L, \quad (15)$$

where $\boldsymbol{\eta}_L = \mathrm{col}(\boldsymbol{\eta}_{kd})$, $k\in\mathcal{V}_L$; $\boldsymbol{\mathcal{L}}_1 = \boldsymbol{\mathcal{D}}_1-\boldsymbol{\mathcal{A}}_1$ and $\boldsymbol{\mathcal{L}}_2 = -\boldsymbol{\mathcal{A}}_2$. Noting that $\boldsymbol{\mathcal{D}}_1$ is a diagonal matrix with positive diagonal elements, and $\boldsymbol{\mathcal{A}}_1$ is a non-negative symmetric matrix with diagonal elements being 0. Then, it gets that $\boldsymbol{\mathcal{L}}_1$ is a nonsingular M-matrix. Therefore, it renders there exists a $M\times M$ diagonal matrix $\boldsymbol{P}_2 = \mathrm{diag}(p_{21},\ldots,p_{2M})$ with $p_{2i}>0$, $i\in\mathcal{V}_F$ such that

$$\boldsymbol{\mathcal{L}}_1^T\boldsymbol{P}_2+\boldsymbol{P}_2\boldsymbol{\mathcal{L}}_1>0. \quad (16)$$

Letting $\boldsymbol{\nabla}(\boldsymbol{\eta}_F)=\boldsymbol{0}_{3M}$, the Nash equilibrium $\boldsymbol{\eta}_F^*$ of noncooperative game for containment (13) is presented as below

$$\boldsymbol{\eta}_F^* = -[\boldsymbol{\mathcal{L}}_1^{-1}\boldsymbol{\mathcal{L}}_2\otimes\boldsymbol{I}_3]\boldsymbol{\eta}_L. \quad (17)$$

To seek the Nash Equilibrium of objective function (13) for multiple ASVs, an IESO-based noncooperative containment controller is derived as

$$\begin{aligned}\boldsymbol{\tau}_i =& -k_i\boldsymbol{M}_i\boldsymbol{R}_i^T[\boldsymbol{R}_i\boldsymbol{\nu}_i+\boldsymbol{\ell}_i\dot{\boldsymbol{\eta}}_L+\boldsymbol{\nabla}_i(\boldsymbol{\eta}_F)]\\ &-\boldsymbol{M}_i\boldsymbol{R}_i^T\dot{\boldsymbol{R}}_i\boldsymbol{\nu}_i-\boldsymbol{M}_i\hat{\boldsymbol{z}}_i,\end{aligned} \quad (18)$$

where $\boldsymbol{\ell}_i\in\Re^{3\times 3(N-M)}$ is the ith row vector of $\boldsymbol{\mathcal{L}}_1^{-1}\boldsymbol{\mathcal{L}}_2\otimes\boldsymbol{I}_3$ satisfying $[\boldsymbol{\ell}_1^T,...,\boldsymbol{\ell}_M]^T=\boldsymbol{\mathcal{L}}_1^{-1}\boldsymbol{\mathcal{L}}_2\otimes\boldsymbol{I}_3$. k_i denotes the designed control gain.

For clarify, we define the column vectors $\boldsymbol{\nu}_F = \mathrm{col}(\boldsymbol{\nu}_i)$, $i\in\mathcal{V}_F$, $\boldsymbol{\tau}_F = \mathrm{col}(\boldsymbol{\tau}_i)$, $i\in\mathcal{V}_F$, $\hat{\boldsymbol{z}}_F = \mathrm{col}(\hat{\boldsymbol{z}}_i)$, $i\in\mathcal{V}_F$, $\tilde{\boldsymbol{z}}_F = \mathrm{col}(\tilde{\boldsymbol{z}}_i)$, $i\in\mathcal{V}_F$, and the block diagonal matrices $\boldsymbol{R}_F = \mathrm{diag}(\boldsymbol{R}_i)$, $i\in\mathcal{V}_F$, $\boldsymbol{M}_F=\mathrm{diag}(\boldsymbol{M}_i)$, $i\in\mathcal{V}_F$, $\boldsymbol{K}=\mathrm{diag}(\boldsymbol{k}_i)$, $i\in\mathcal{V}_F$. Based on the designed IESO (7) and controller (18), one has

$$\begin{aligned}\dot{\boldsymbol{\eta}}_F &= \boldsymbol{R}_F\boldsymbol{\nu}_F,\\ \dot{\boldsymbol{\nu}}_F &= -\boldsymbol{R}_F^T\boldsymbol{K}[\boldsymbol{R}_F\boldsymbol{\nu}_F+(\boldsymbol{\mathcal{L}}_1^{-1}\boldsymbol{\mathcal{L}}_2\otimes\boldsymbol{I}_3)\dot{\boldsymbol{\eta}}_L\\ &\quad+\boldsymbol{\nabla}(\boldsymbol{\eta}_F)]-\boldsymbol{R}_F^T\dot{\boldsymbol{R}}_F\boldsymbol{\nu}_F-\tilde{\boldsymbol{z}}_F.\end{aligned} \quad (19)$$

3.3 Convergence Analysis

In the previous subsections, it derived the IESO-based noncooperative containment controller for ASVs subject to unknown disturbances. In the forthcoming, the convergence results is given by the following theorem.

Theorem 1: Consider the noncooperative game (4) and (5) described by multiple ASVs with the action dynamics (1), the IESO (7), and the noncooperative containment controller (18). Under Assumptions 1-3, the closed-loop system is input-to-state stable, and the states of ASVs converge to the neighborhood of the time-varying NE solutions.

Proof: Construct a Lyapunov function candidate V as

$$V = V_1+V_2, \quad (20)$$

$$V_1 = (\boldsymbol{\eta}_F-\boldsymbol{\eta}_F^*)^T(\boldsymbol{P}_2\otimes\boldsymbol{I}_3)(\boldsymbol{\eta}_F-\boldsymbol{\eta}_F^*), \quad (21)$$

$$V_2 = \frac{1}{2}\|\boldsymbol{R}_F\boldsymbol{\nu}_F+(\boldsymbol{\mathcal{L}}_1^{-1}\boldsymbol{\mathcal{L}}_2\otimes I_3)\dot{\boldsymbol{\eta}}_L+\boldsymbol{\nabla}(\boldsymbol{\eta}_F)\|^2. \quad (22)$$

By differentiating V_1 along (19) and substituting $\boldsymbol{\nabla}(\boldsymbol{\eta}_F)$ and $\boldsymbol{\nabla}(\boldsymbol{\eta}_F^*)$, it follows

$$\begin{aligned}\dot{V}_1 =& (\boldsymbol{\eta}_F-\boldsymbol{\eta}_F^*)^T(\boldsymbol{P}_2\otimes\boldsymbol{I}_3)[\boldsymbol{R}_F\boldsymbol{\nu}_F+(\boldsymbol{\mathcal{L}}_1^{-1}\boldsymbol{\mathcal{L}}_2\otimes\boldsymbol{I}_3)\dot{\boldsymbol{\eta}}_L]\\ &+[\boldsymbol{R}_F\boldsymbol{\nu}_F+(\boldsymbol{\mathcal{L}}_1^{-1}\boldsymbol{\mathcal{L}}_2\otimes\boldsymbol{I}_3)\dot{\boldsymbol{\eta}}_L]^T(\boldsymbol{P}_2\otimes\boldsymbol{I}_3)(\boldsymbol{\eta}_F-\boldsymbol{\eta}_F^*)\\ =& (\boldsymbol{\eta}_F-\boldsymbol{\eta}_F^*)^T(\boldsymbol{P}_2\otimes\boldsymbol{I}_3)[\boldsymbol{R}_F\boldsymbol{\nu}_F+(\boldsymbol{\mathcal{L}}_1^{-1}\boldsymbol{\mathcal{L}}_2\otimes\boldsymbol{I}_3)\dot{\boldsymbol{\eta}}_L\\ &+\boldsymbol{\nabla}(\boldsymbol{\eta}_F)]+[\boldsymbol{R}_F\boldsymbol{\nu}_F+(\boldsymbol{\mathcal{L}}_1^{-1}\boldsymbol{\mathcal{L}}_2\otimes I_3)\dot{\boldsymbol{\eta}}_L+\boldsymbol{\nabla}(\boldsymbol{\eta}_F)]^T\\ &\times(\boldsymbol{P}_2\otimes\boldsymbol{I}_3)(\boldsymbol{\eta}_F-\boldsymbol{\eta}_F^*)\\ &-(\boldsymbol{\eta}_F-\boldsymbol{\eta}_F^*)^T(\boldsymbol{P}_2\otimes\boldsymbol{I}_3)[\boldsymbol{\nabla}(\boldsymbol{\eta}_F)-\boldsymbol{\nabla}(\boldsymbol{\eta}_F^*)]\\ &-[\boldsymbol{\nabla}(\boldsymbol{\eta}_F)-\boldsymbol{\nabla}(\boldsymbol{\eta}_F^*)]^T(\boldsymbol{P}_2\otimes\boldsymbol{I}_3)(\boldsymbol{\eta}_F-\boldsymbol{\eta}_F^*).\end{aligned} \quad (23)$$

Note that we have $\boldsymbol{\nabla}(\boldsymbol{\eta}_F)-\boldsymbol{\nabla}(\boldsymbol{\eta}_F^*)=(\boldsymbol{\mathcal{L}}_1\otimes\boldsymbol{I}_3)(\boldsymbol{\eta}_F-\boldsymbol{\eta}_F^*)$ by (19) and (17). Thus, it yields

$$\begin{aligned}&-(\boldsymbol{\eta}_F-\boldsymbol{\eta}_F^*)^T(\boldsymbol{P}_2\otimes\boldsymbol{I}_3)[\boldsymbol{\nabla}(\boldsymbol{\eta}_F)-\boldsymbol{\nabla}(\boldsymbol{\eta}_F^*)]\\ &-[\boldsymbol{\nabla}(\boldsymbol{\eta}_F)-\boldsymbol{\nabla}(\boldsymbol{\eta}_F^*)]^T(\boldsymbol{P}_2\otimes\boldsymbol{I}_3)(\boldsymbol{\eta}_F-\boldsymbol{\eta}_F^*)\\ =&-(\boldsymbol{\eta}_F-\boldsymbol{\eta}_F^*)^T[(\boldsymbol{P}_2\boldsymbol{\mathcal{L}}_1+\boldsymbol{\mathcal{L}}_1^T\boldsymbol{P}_2)\otimes\boldsymbol{I}_3](\boldsymbol{\eta}_F-\boldsymbol{\eta}_F^*)\\ \le&-\gamma_1\|\boldsymbol{\eta}_F-\boldsymbol{\eta}_F^*\|^2,\end{aligned} \quad (24)$$

with $\gamma_1=\lambda_{\min}(\boldsymbol{P}\boldsymbol{\mathcal{L}}_1+\boldsymbol{\mathcal{L}}_1^T\boldsymbol{P})$.

Further, we have

$$\begin{aligned}\dot{V}_1 \le& -\gamma_1\|\boldsymbol{\eta}_F-\boldsymbol{\eta}_F^*\|^2+2\lambda_{\max}(\boldsymbol{P}_2)\|\boldsymbol{\eta}_F-\boldsymbol{\eta}_F^*\|\\ &\times\|\boldsymbol{R}_F\boldsymbol{\nu}_F+(\boldsymbol{\mathcal{L}}_1^{-1}\boldsymbol{\mathcal{L}}_2\otimes I_3)\dot{\boldsymbol{\eta}}_L+\boldsymbol{\nabla}(\boldsymbol{\eta}_F)\|.\end{aligned} \quad (25)$$

Then, we proceed to calculate the derivative of V_2. Integrating (15) and (19), $\dot{V}_2$ is presented as follows

$$\begin{aligned}\dot{V}_2 =& -\lambda_{\min}(\boldsymbol{K})\|\boldsymbol{R}_F\boldsymbol{\nu}_F+(\boldsymbol{\mathcal{L}}_1^{-1}\boldsymbol{\mathcal{L}}_2\otimes\boldsymbol{I}_3)\dot{\boldsymbol{\eta}}_L+\boldsymbol{\nabla}(\boldsymbol{\eta}_F)\|^2\\ &+[\boldsymbol{R}_F\boldsymbol{\nu}_F+(\boldsymbol{\mathcal{L}}_1^{-1}\boldsymbol{\mathcal{L}}_2\otimes\boldsymbol{I}_3)\dot{\boldsymbol{\eta}}_L+\boldsymbol{\nabla}(\boldsymbol{\eta}_F)]^T\\ &\times[(\boldsymbol{\mathcal{L}}_1\otimes\boldsymbol{I}_3)\boldsymbol{R}_F\boldsymbol{\nu}_F+(\boldsymbol{\mathcal{L}}_2\otimes\boldsymbol{I}_3)\dot{\boldsymbol{\eta}}_L\\ &+(\boldsymbol{\mathcal{L}}_1^{-1}\boldsymbol{\mathcal{L}}_2\otimes\boldsymbol{I}_3)\ddot{\boldsymbol{\eta}}_L-\boldsymbol{R}_F\tilde{\boldsymbol{z}}_F].\end{aligned} \quad (26)$$

From Lemma 1, it gets $\|\tilde{\boldsymbol{z}}_i\|\le\sigma^*\in\Re^+$. Under Assump-

Authorized licensed use limited to: Shanghai Jiaotong University. Downloaded on December 22,2024 at 11:13:09 UTC from IEEE Xplore. Restrictions apply.

tions 1-3, the following inequalities can be obtained

$$\begin{aligned}&[\boldsymbol{R}_F\boldsymbol{\nu}_F+(\boldsymbol{\mathcal{L}}_1^{-1}\boldsymbol{\mathcal{L}}_2\otimes\boldsymbol{I}_3)\dot{\boldsymbol{\eta}}_L+\boldsymbol{\nabla}(\boldsymbol{\eta}_F)]^T\\&\times[(\boldsymbol{\mathcal{L}}_1^{-1}\boldsymbol{\mathcal{L}}_2\otimes\boldsymbol{I}_3)\ddot{\boldsymbol{\eta}}_L-\boldsymbol{R}_F\tilde{\boldsymbol{z}}_F]\\&\leq\|\boldsymbol{R}_F\boldsymbol{\nu}_F+(\boldsymbol{\mathcal{L}}_1^{-1}\boldsymbol{\mathcal{L}}_2\otimes\boldsymbol{I}_3)\dot{\boldsymbol{\eta}}_L+\boldsymbol{\nabla}(\boldsymbol{\eta}_F)\|\\&\times\left[\|(\boldsymbol{\mathcal{L}}_1^{-1}\boldsymbol{\mathcal{L}}_2\otimes\boldsymbol{I}_3)\ddot{\boldsymbol{\eta}}_L\|+\|\tilde{\boldsymbol{z}}_F\|\right]\\&\leq\|\boldsymbol{R}_F\boldsymbol{\nu}_F+(\boldsymbol{\mathcal{L}}_1^{-1}\boldsymbol{\mathcal{L}}_2\otimes\boldsymbol{I}_3)\dot{\boldsymbol{\eta}}_L+\boldsymbol{\nabla}(\boldsymbol{\eta}_F)\|\\&\times(\sqrt{N-M}\epsilon_3+\sqrt{M}\sigma^*).\end{aligned}\tag{27}$$

Similarly, using $\boldsymbol{\nabla}(\boldsymbol{\eta}_F)-\boldsymbol{\nabla}(\boldsymbol{\eta}_F^*)=(\boldsymbol{\mathcal{L}}_1\otimes\boldsymbol{I}_3)(\boldsymbol{\eta}_F-\boldsymbol{\eta}_F^*)$, one has

$$\begin{aligned}\dot{V}_2=&-(\lambda_{\min}(\boldsymbol{K})-\varpi)\|\boldsymbol{R}_F\boldsymbol{\nu}_F+(\boldsymbol{\mathcal{L}}_1^{-1}\boldsymbol{\mathcal{L}}_2\otimes\boldsymbol{I}_3)\dot{\boldsymbol{\eta}}_L\\&+\boldsymbol{\nabla}(\boldsymbol{\eta}_F)\|^2+\varpi^2\|\boldsymbol{\eta}_F-\boldsymbol{\eta}_F^*\|\|\boldsymbol{R}_F\boldsymbol{\nu}_F+\boldsymbol{\nabla}(\boldsymbol{\eta}_F)\\&+(\boldsymbol{\mathcal{L}}_1^{-1}\boldsymbol{\mathcal{L}}_2\otimes\boldsymbol{I}_3)\dot{\boldsymbol{\eta}}_L\|+(\sqrt{N-M}\epsilon_3+\sqrt{M}\sigma^*)\\&\times\|\boldsymbol{R}_F\boldsymbol{\nu}_F+(\boldsymbol{\mathcal{L}}_1^{-1}\boldsymbol{\mathcal{L}}_2\otimes\boldsymbol{I}_3)\dot{\boldsymbol{\eta}}_L+\boldsymbol{\nabla}(\boldsymbol{\eta}_F)\|\end{aligned}\tag{28}$$

with $\varpi=\|\boldsymbol{\mathcal{L}}_1\otimes\boldsymbol{I}_3\|$.

Based on the above results (24) and (28), the derivative of V is given as

$$\begin{aligned}\dot{V}=&\dot{V}_1+\dot{V}_2\\&\leq-\gamma_1\|\boldsymbol{\eta}_F-\boldsymbol{\eta}_F^*\|^2-(\lambda_{\min}(\boldsymbol{K})-\varpi)\|\boldsymbol{R}_F\boldsymbol{\nu}_F\\&+(\boldsymbol{\mathcal{L}}_1^{-1}\boldsymbol{\mathcal{L}}_2\otimes\boldsymbol{I}_3)\dot{\boldsymbol{\eta}}_L+\boldsymbol{\nabla}(\boldsymbol{\eta}_F)\|^2+(2\lambda_{\max}(\boldsymbol{P}_2)+\varpi^2)\\&\times\|\boldsymbol{\eta}_F-\boldsymbol{\eta}_F^*\|\|\boldsymbol{R}_F\boldsymbol{\nu}_F+(\boldsymbol{\mathcal{L}}_1^{-1}\boldsymbol{\mathcal{L}}_2\otimes I_3)\dot{\boldsymbol{\eta}}_L+\boldsymbol{\nabla}(\boldsymbol{\eta}_F)\|\\&+(\sqrt{N-M}\epsilon_3+\sqrt{M}\sigma^*)\|\boldsymbol{R}_F\boldsymbol{\nu}_F\\&+(\boldsymbol{\mathcal{L}}_1^{-1}\boldsymbol{\mathcal{L}}_2\otimes\boldsymbol{I}_3)\dot{\boldsymbol{\eta}}_L+\boldsymbol{\nabla}(\boldsymbol{\eta}_F)\|.\end{aligned}\tag{29}$$

Letting $\boldsymbol{E}_2=\left[\|\boldsymbol{\eta}_F-\boldsymbol{\eta}_F^*\|,\|\boldsymbol{R}_F\boldsymbol{\nu}_F+(\boldsymbol{\mathcal{L}}_1^{-1}\boldsymbol{\mathcal{L}}_2\otimes I_3)\dot{\boldsymbol{\eta}}_L+\boldsymbol{\nabla}(\boldsymbol{\eta}_F)\|\right]^T$, one has

$$\dot{V}\leq-\boldsymbol{E}_2^T\boldsymbol{A}_2\boldsymbol{E}_2+\boldsymbol{B}_2\boldsymbol{E}_2\tag{30}$$

where

$$\boldsymbol{A}_2=\begin{bmatrix}\gamma_1 & -\dfrac{\lambda_{\max}(\boldsymbol{P}_2)+\varpi^2}{2}\\ -\dfrac{\lambda_{\max}(\boldsymbol{P}_2)+\varpi^2}{2} & \lambda_{\min}(\boldsymbol{K})-\varpi\end{bmatrix},$$

$$\boldsymbol{B}_2=\begin{bmatrix}0\\ \sqrt{N-M}\epsilon_3+\sqrt{M}\sigma^*\end{bmatrix}.$$

For $\lambda_{\min}(\boldsymbol{K})>(\lambda_{\max}(\boldsymbol{P}_2)+\varpi^2)^2/4\gamma_1+\varpi$, it gets that $\boldsymbol{A}_2$ is positive definite. Then, $\dot{V}$ satisfies

$$\dot{V}\leq-\lambda_{\min}(\boldsymbol{A}_2)\|\boldsymbol{E}_2\|^2+\|\boldsymbol{B}_2\|\|\boldsymbol{E}_2\|.\tag{31}$$

Since $\|\boldsymbol{E}_2\|\geq\|\boldsymbol{B}_2\|/\varrho\lambda_{\min}(\boldsymbol{A}_2)$ with $\varrho\in\Re^+$, it follows

$$\dot{V}\leq-\lambda_{\min}(\boldsymbol{A}_2)(1-\varrho)\|\boldsymbol{E}_2\|^2.\tag{32}$$

Therefore, it can be concluded that the proposed closed-loop system is input-to-state stable, and error signals are bounded.

4 Simulation Results

This section considers the noncooperative containment control of three ASVs and four virtual leaders. Fig. 1 displays the communication topology and a desired containment shape of ASVs and virtual leaders using the presented IESO-based noncooperative containment control scheme.

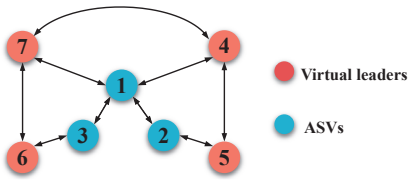

Fig. 1: The communication topology and the desired containment shape.

In [24], the model parameters of ASVs can be found, and ASVs' initial states are set at $[-50,-50,\pi/2,0,0,0]^T$, $[-60,-50,\pi/2,0,0,0]^T$, and $[-40,-50,\pi/2,0,0,0]^T$, successively. The reference trajectories for virtual leaders are defined by $[x_{kd},y_{kd}]=[-10-0.2t+80\cos(-0.4t/80+5\pi/4),20+0.1t+80\sin(-0.4t/80+5\pi/4)]$, $k=4,7$ and $[x_{kd},y_{kd}]=[-10-0.2(t-50)+80\cos(-0.4(t-50)/80+5\pi/4),20+0.1(t-50)+80\sin(-0.4(t-50)/80+5\pi/4)]$, $k=5,6$. Other parameters are $l_{i1}=5$, $l_{i2}=100$, $b_0=0.5$, $c_0=2$, and $k_i=1$.

Simulation results are plotted in Figs. 2-11. Fig. 2 draws the actual trajectories of ASVs and virtual leaders using presented method. Figs. 3-5 shows the errors between ASVs' states and Nash equilibrium solutions. Figs. 6-8 depicts the actual control inputs. Figs. 9-11 display the estimation profiles of designed IESO.

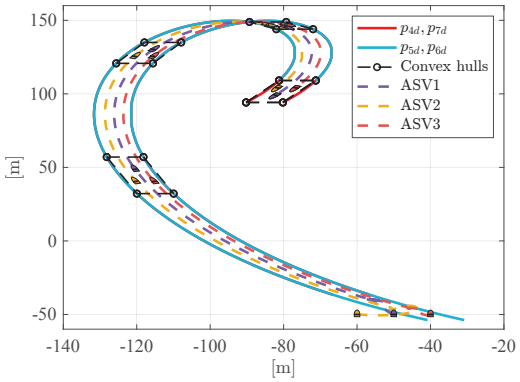

Fig. 2: The actual trajectories of 3 ASVs.

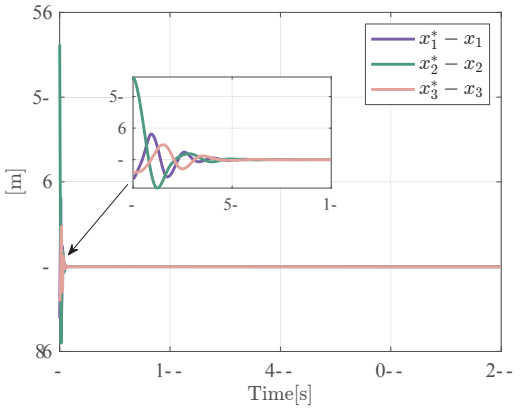

Fig. 3: Deviations of x_i and x_i^*.

5 Conclusion

This paper addressed the problem of distributed containment control for ASVs in the presence of internal and ex-

Authorized licensed use limited to: Shanghai Jiaotong University. Downloaded on December 22,2024 at 11:13:09 UTC from IEEE Xplore. Restrictions apply.

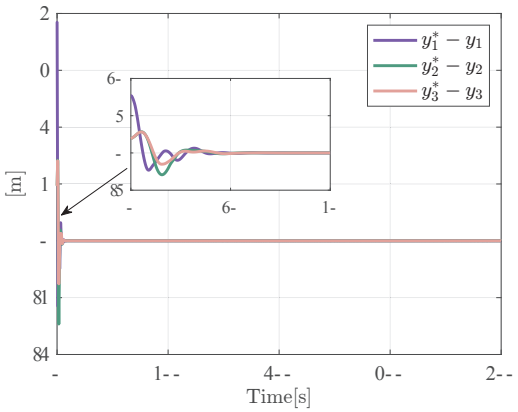

Fig. 4: Deviations of y_i and y_i^*.

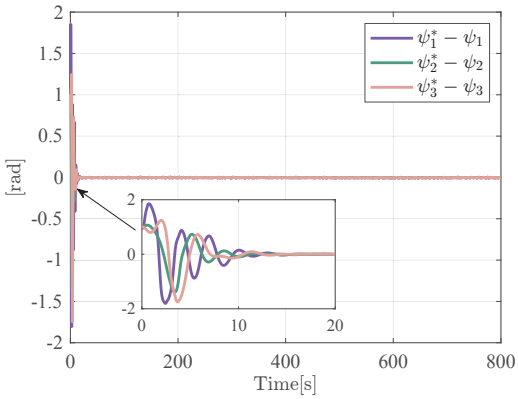

Fig. 5: Deviations of ψ_i and ψ_i^*.

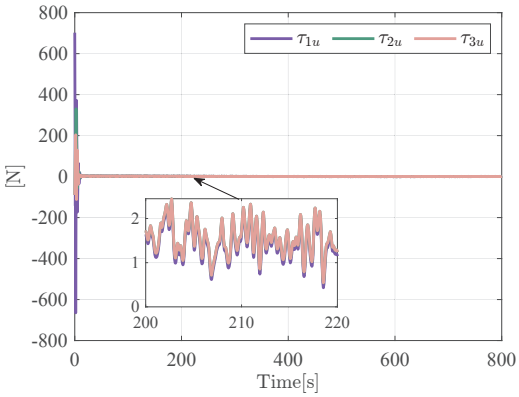

Fig. 6: The surge control inputs.

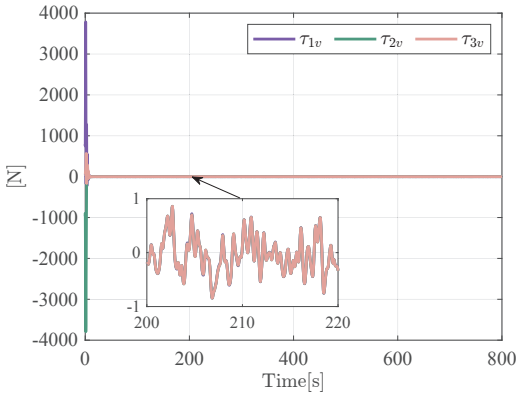

Fig. 7: The sway control inputs.

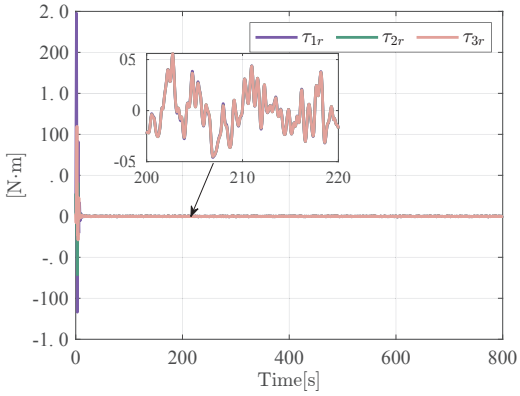

Fig. 8: The yaw control inputs.

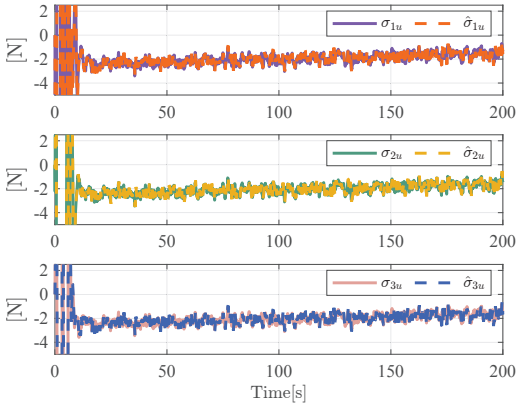

Fig. 9: Estimation profiles of IESO in the surge direction.

ternal disturbances. By considering ASVs with individual tasks, a noncooperative game-based control scheme was developed to achieve the desired containment behavior. To handle the disturbances, an IESO was designed. By employing a Nash equilibrium seeking strategy, an IESO-based noncooperative containment controller was presented. The analysis demonstrated that the closed-loop system is input-to-state stable, and the position and heading of all ASVs converge to the Nash equilibrium to the greatest extent possible. The effectiveness of the proposed scheme was illustrated through simulation results. Overall, this research contributes to advancing the field of distributed containment control for ASVs and provides a practical solution for dealing with disturbances in real-world scenarios.

References

[1] Y. Shi, C. Shen, H. Fang, and H. Li, "Advanced control in marine mechatronic systems: A survey," *IEEE/ASME Transactions on Mechatronics*, vol. 22, no. 7, pp. 1121–1131, Jan 2017.

[2] N. Gu, D. Wang, Z. Peng, J. Wang, and Q.-L. Han, "Advances in line-of-sight guidance for path following of autonomous marine vehicles: An overview," *IEEE Transactions on Systems, Man, and Cybernetics: Systems*, vol. 53, no. 1, pp. 12–28, 2023.

[3] Z. Jia, Z. Hu, and W. Zhang, "Adaptive output-feedback control with prescribed performance for trajectory tracking of underactuated surface vessels," *ISA Transactions*, vol. 95, pp. 18–26, 2019.

[4] W. Wu, Z. Peng, D. Wang, L. Liu, and N. Gu, "Anti-

Authorized licensed use limited to: Shanghai Jiaotong University. Downloaded on December 22,2024 at 11:13:09 UTC from IEEE Xplore. Restrictions apply.

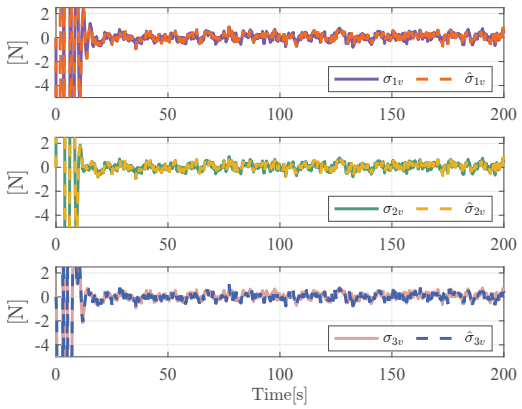

Fig. 10: Estimation profiles of IESO in the sway direction.

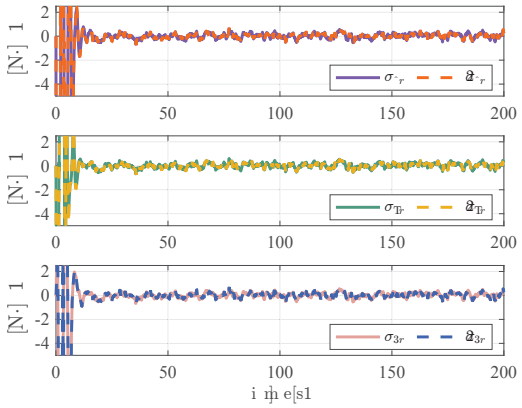

Fig. 11: Estimation profiles of IESO in the yaw direction.

disturbance leader–follower synchronization control of marine vessels for underway replenishment based on robust exact differentiators," *Ocean Engineering*, vol. 248, p. 110686, 2022.

[5] W. Wu, Z. Peng, D. Wang, L. Liu, and Q.-L. Han, "Network-based line-of-sight path tracking of underactuated unmanned surface vehicles with experiment results," *IEEE Transactions on Cybernetics*, vol. 52, no. 10, pp. 10 937 – 10 947, 2022.

[6] W. Wu, Z. Peng, L. Liu, and D. Wang, "A general safety-certified cooperative control architecture for interconnected intelligent surface vehicles with applications to vessel train," *IEEE Transaction on Intelligent Vehicle*, vol. 7, no. 3, pp. 627–637, 2022.

[7] Z. Peng, J. Wang, D. Wang, and Q.-L. Han, "An overview of recent advances in coordinated control of multiple autonomous surface vehicles," *IEEE Transactions on Industrial Informatics*, vol. 17, no. 2, pp. 732–745, 2021.

[8] Y. Zhang, D. Wang, and Z. Peng, "Consensus maneuvering for a class of nonlinear multivehicle systems in strict-feedback form," *IEEE Transactions on Cybernetics*, vol. 49, no. 5, pp. 1759–1767, 2019.

[9] Z. Peng, J. Wang, and D. Wang, "Distributed maneuvering of autonomous surface vehicles based on neurodynamic optimization and fuzzy approximation," *IEEE Transactions on Control Systems Technology*, vol. 26, no. 3, pp. 1083–1090, 2018.

[10] W. Wu, Y. Zhang, W. Zhang, and W. Xie, "Distributed finite-time performance-prescribed time-varying formation control of autonomous surface vehicles with saturated inputs," *Ocean Engineering*, vol. 266, Oct. 2022, doi: 10.1016/j.oceaneng.2022.112866.

[11] W. Wang, D. Wang, and Z. Peng, "Fault-tolerant containment control of uncertain nonlinear systems in strict-feedback form," *International Journal of Robust and Nonlinear Control*, vol. 27, no. 3, pp. 497–511, 2017.

[12] Z. Li, W. Ren, X. Liu, and M. Fu, "Distributed containment control of multi-agent systems with general linear dynamics in the presence of multiple leaders," *International Journal of Robust and Nonlinear Control*, vol. 23, no. 5, pp. 534–547, 2013.

[13] Y. Zheng and L. Wang, "Containment control of heterogeneous multi-agent systems," *International Journal of Control*, vol. 87, no. 1, pp. 1–8, 2014.

[14] Y. Zhang, D. Wang, Z. Peng, T. Li, and L. Liu, "Event-triggered ISS-modular neural network control for containment maneuvering of nonlinear strict-feedback multi-agent systems," *Neurocomputing*, vol. 377, pp. 314–324, 2020.

[15] N. Gu, D. Wang, Z. Peng, and L. Liu, "Observer-based finite-time control for distributed path maneuvering of underactuated unmanned surface vehicles with collision avoidance and connectivity preservation," *IEEE Transactions on Systems, Man, and Cybernetics: Systems*, vol. 51, no. 8, pp. 5105–5115, Aug. 2019.

[16] N. Gu, D. Wang, Z. Peng, and J. Wang, "Safety-critical containment maneuvering of underactuated autonomous surface vehicles based on neurodynamic optimization with control barrier functions," *IEEE Transactions on Neural Networks and Learning Systems*, vol. 34, no. 6, pp. 2882–2895, 2023.

[17] Y. Zhang, D. Wang, Z. Peng, and T. Li, "Distributed containment maneuvering of uncertain multiagent systems in mimo strict-feedback form," *IEEE Transactions on Systems, Man, and Cybernetics: Systems*, vol. 51, no. 2, pp. 1354–1364, 2021.

[18] M. Ye and G. Hu, "Distributed nash equilibrium seeking by a consensus based approach," *IEEE Transactions on Automatic Control*, vol. 62, no. 9, pp. 4811–4818, 2017.

[19] X. Fang, J. Zhou, and G. Wen, "Location game of multiple unmanned surface vessels with quantized communications," *IEEE Transactions on Circuits and Systems II: Express Briefs*, vol. 69, no. 3, pp. 1322–1326, 2022.

[20] X. Fang, G. Wen, X. Yu, and G. Chen, "Formation control for unmanned surface vessels: A game-theoretic approach," *Asian Journal of Control*, vol. 24, no. 2, pp. 498–509, 2022.

[21] Y. Zhang, W. Wu, and W. Zhang, "Noncooperative game-based cooperative maneuvering of intelligent surface vehicles via accelerated learning-based neural predictors," *IEEE Transaction on Intelligent Vehicle*, vol. 8, no. 3, pp. 2212–2221, 2023.

[22] N. Gu, H. Wang, A. Wang, and L. Liu, "Safety-critical game-based formation control of underactuated autonomous surface vehicles," *IEEE/CAA Journal of Automatica Sinica*, vol. 10, no. 4, pp. 1102–1104, 2023.

[23] Z. Zhang, Y. Guo, D. Gong, and J. Liu, "Global integral sliding-mode control with improved nonlinear extended state observer for rotary tracking of a hydraulic roofbolter," *IEEE/ASME Transactions on Mechatronics*, vol. 28, no. 1, pp. 483–494, 2023.

[24] R. Skjetne, T. I. Fossen, and P. V. Kokotović, "Adaptive maneuvering, with experiments, for a model ship in a marine control laboratory," *Automatica*, vol. 41, no. 2, pp. 289–298, Feb. 2005.

Authorized licensed use limited to: Shanghai Jiaotong University. Downloaded on December 22,2024 at 11:13:09 UTC from IEEE Xplore. Restrictions apply.